

The solvation dynamics of Na⁺ and K⁺ ions in liquid methanol

Cristian Faralli · Marco Pagliai · Gianni Cardini ·
Vincenzo Schettino

Received: 19 September 2006 / Accepted: 1 March 2007 / Published online: 18 April 2007
© Springer-Verlag 2007

Abstract The structure of the solvation shell of Na⁺ and K⁺ in fully deuterated liquid methanol has been studied by ab initio Car-Parrinello molecular dynamics simulations. The solvent cage has been found relatively stable and this property has been explained by means of charge transfer and electrostatic interactions as was previously done for Li⁺ in the same solvent. The differences with Li⁺ such as the increase of the coordination number going from Li⁺ to K⁺ and the reduced stability of the cage have been ascribed to the increase in the ionic radius.

Introduction

Ion solvation [1] plays an important role in chemical reaction mechanisms in solution. Alkaline and alkaline-earth ions, of particular interest in many biochemical processes, have been the object of extended experimental and theoretical studies to understand the nature of their interactions with solvent molecules and the structure and stability of their solvation shells [2]. To study the ion solvation, especially in water, many experimental methods have been applied including neutron and X-ray scattering, infrared and Raman spectroscopy and, more recently, femtosecond spectroscopy [3–6]. On the other hand, it has been proved that computational and theoretical methods are powerful tools to give insights also into properties difficult to be addressed experimentally. Many of

these studies have dealt with alkaline ions in water [2, 7–18] showing the key role of polarization interactions and charge transfer [14, 18–23]. Only a more limited attention has been devoted to ions solvation in other solvents such as methanol [22–27], acetonitrile [28], tetrahydrofuran [25] or acetone [29, 30] and in some cases the knowledge of some important properties of the first solvation shell is still incomplete.

Molecular dynamics (MD) [31–33] and Monte Carlo simulations [19, 25, 34] are particularly suited to study the several aspects of ion solvation. In the classical approach, based on semiempirical potentials, simulation methods are unable to correctly reproduce the “experimental” coordination number particularly when charge transfer and polarization effects are at work [19–21, 32, 35, 36]. These problems are to a good extent overcome by first principles molecular dynamics simulations that explicitly take the fluctuations of the electron density into account and by QM/MM methods that allow to treat a small part of the system to an high level of theory and treating the rest of the system with semiempirical potential to reduce the system-size limitations. In the present work the structural and dynamical aspects of the Na⁺ and K⁺ ions solvation in liquid methanol have been studied with Car-Parrinello molecular dynamics simulations (CPMD) [37, 38]. Methanol is of interest by itself [39–41] as the simplest organic solvent with a hydrophobic (CH₃) and a hydrophilic (OH) group. The methanol interaction with anions mainly involves hydrogen bonding [22, 23] while the interaction with cations is predominantly electrostatic. However, in a previous work [22] it has been shown that in the solvation process of Li⁺ in methanol the charge transfer and polarization effects are significant. Extension of the ab initio simulations to Na⁺ and K⁺ solvation will allow to draw a more complete picture of the solvation process of alkaline ions as a function of the ion dimension. Solvations of Na⁺ and K⁺ have been studied with success in water by QM/MM

C. Faralli · M. Pagliai · G. Cardini (✉) · V. Schettino
Laboratorio di Spettroscopia Molecolare,
Dipartimento di Chimica, Università di Firenze,
Via della Lastruccia 3, 50019 Sesto Fiorentino, Firenze, Italy
e-mail: gianni.cardini@unifi.it

G. Cardini · V. Schettino
European Laboratory for Nonlinear Spectroscopy (LENS),
via Nello Carrara 1, 50019 Sesto Fiorentino, Firenze, Italy

simulations [42] and Car-Parrinello molecular dynamics [43,44] but is still lacking in other solvents like methanol.

Computational details

The simulations have been performed with the CPMD code [45] in a cubic box of 12.05 Å side, with periodic boundary conditions and 25 methanol molecules and one ion. The Na⁺ solution has been studied starting from a configuration of a previous CPMD simulation on Li⁺ in fully deuterated liquid methanol [22]. As in previous papers [22,23,39] the use of the deuterium isotope was adopted to allow for a larger time step. The starting configuration for the K⁺ solution has been obtained by substituting the sodium with the potassium ion. The simulations in this work have been performed adopting Martins-Troullier (MT) [46] pseudopotentials along with the Kleinman-Bylander [47] decomposition for the C and O atoms, whereas a Von Barth-Car [17] pseudopotential has been adopted for the H atoms; this choice has been shown to give good results for pure liquid methanol [39]. Relativistic, norm-conserving, separable, dual-space semicore (9 electrons have been treated explicitly) pseudopotentials of Goedecker, Teter, Hutter (GTH) type [48–50] have been used for the ions to give both structural and electronic satisfactory results. The same choice was made in the previous study for Li⁺ [22]. Calculations with a Martins-Troullier (MT) pseudopotential [46] have been also performed for comparison on the structural properties and the results are in the expected agreement for this kind of simulations [51].

The plane wave expansion has been truncated at 70 Ry, following previous studies on liquid methanol [39] and on ions in methanol [22,23]. This choice allows for a good convergence on the binding energy as shown in Table 1.

Density functional calculations in the generalized gradient approximation (GGA) have been performed using the BLYP [52,53] exchange-correlation functional. In order to validate the computational strategy adopted, the structure of the CH₃OH complex with Na⁺ and K⁺ has been calculated with our approach and compared to DFT and MP2 calculations with a localized gaussian basis set, 6-311++G(3df,3pd), adopting the Gaussian 98 suite of programs [54]. The results, summarized in Table 2, show that the BLYP functional in conjunction with the plane wave basis set satisfactory reproduces the structural parameters of the complexes.

A fictitious electronic mass of 800 a.u. has been adopted to keep the system on the Born–Oppenheimer surface. After a thermalization at 300 K by velocity scaling, the equation of motions have been integrated with a time step of 5 a.u. (~0.12 fs) for a total simulation time of ~ 8 ps in the NVE ensemble, storing the atomic coordinates and velocities at every step for the subsequent analysis. Electron localization properties have been studied through the position of the maximally localized Wannier function centers (WFCs) [55–57] and population analysis has been carried with the Atoms in Molecules (AIM) [58,59] method, that does not show a strong basis set dependence [60]. These calculations were carried averaging over 128 equally time spaced configurations.

Results and discussion

Salient structural data (first peak position and coordination number in the ion–oxygen pair radial distribution functions) obtained in this work with different pseudopotentials are reported in Table 3 and compared with classical MD results. GTH pseudopotentials have been found very effective in the description of the structural and dynamics properties of the Li⁺ in methanol [22] and have been adopted with confidence in this work. Nevertheless, the results on the average description related to the ion solvent interactions have been compared with standard MT [46] pseudopotentials and the results are in the expected agreement for short simulations [51].

The simulations with the GTH pseudopotential have been started from the last configuration obtained by the simulations with the MT pseudopotential and a further thermalization by velocity scaling for at least 1 ps have been applied to the system before the production run.

As in the case of the Li⁺ in liquid methanol [22] the coordination number of the alkali metal ions obtained by CPMD is lower than found by classical MD, suggesting that the charge transfer and polarization effects play an important role in the overall description of the mutual interactions between solute and solvent [22,32,36]. Instead the first peak position in the ion–oxygen pair radial distribution functions appears to be quite independent of the model adopted, in the same way as observed in the CPMD studies of these ions in water [43,44].

Table 1 Binding energy for the complex cation-methanol, obtained after geometry optimization for each plane wave cutoff

Cutoff (Ry)	Na-MeOH (au)	Na-MeOH (kJ/mol)	K-MeOH (au)	K-MeOH (kJ/mol)
60	−0.0398	−104.5	−0.0273	−71.7
70	−0.0406	−106.4	−0.0277	−72.8
80	−0.0405	−106.2	−0.0278	−72.9
90	−0.0405	−106.4	−0.0277	−72.8
100	−0.0404	−106.1	−0.0277	−72.8

Table 2 Salient structural data of the CH₃OH...Na⁺ and CH₃OH...K⁺ complexes

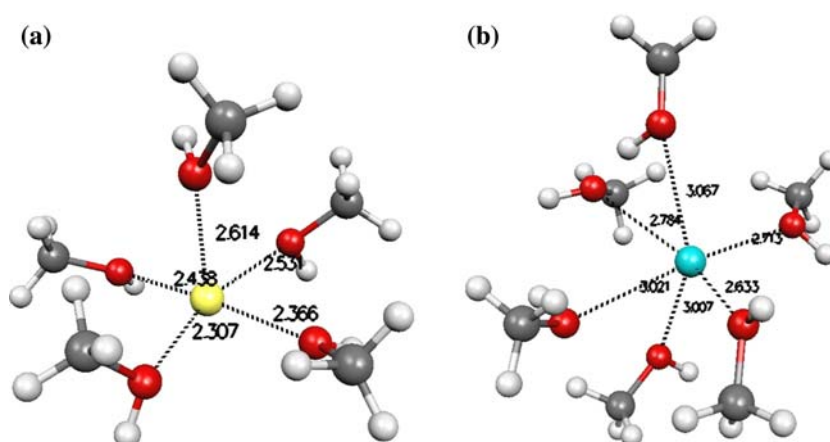
	BLYP/PW	BLYP/G	B3LYP/G	MP2/G
{CH₃OH...Na⁺}				
r _{O...Na}	2.228	2.209	2.193	2.252
r _{O-H}	0.973	0.972	0.962	0.961
r _{O-C}	1.486	1.473	1.452	1.446
<r _{H-C} >	1.091	1.093	1.087	1.085
θ _{Na...O-H}	121.24	123.43	123.29	123.27
θ _{Na...O-C}	131.35	129.07	128.70	129.49
{CH₃OH...K⁺}				
r _{O...K}	2.573	2.607	2.590	2.589
r _{O-H}	0.973	0.972	0.962	0.961
r _{O-C}	1.480	1.467	1.446	1.441
<r _{H-C} >	1.093	1.094	1.088	1.086
θ _{K...O-H}	125.70	123.21	123.21	124.49
θ _{K...O-C}	127.03	129.53	128.96	128.46

Distances are in Å, angles in degrees (for the H–C bond length the average value is reported). G and PW label the calculations with the Gaussian basis sets 6-311++G(3df,3pd) and plane waves expansion, respectively

It is important to note that the coordination number obtained with CPMD simulations for both ions in methanol is lower than the corresponding value in water, essentially due to the greater steric effects of the methanol molecules. In fact the coordination number in water for Na⁺ and K⁺ are 5.2 and 6.75, respectively.

A snapshot of the first solvation shell of the Na⁺ and K⁺ ions is shown in Fig. 1.

The interaction of cations with methanol is mainly electrostatic with the methanol dipole moment pointing toward the ion. In fact in the pair radial distribution functions (shown in Fig. 2) the oxygen atom is the closest to the ions. This implies that the oxygen lone pairs are on the side of the ion and this will favor the charge transfer from the solvent to the ion.

Fig. 1 Snapshot of the first solvation shell for Na⁺ (a) and K⁺ (b)**Table 3** First peak position (Å) and integration number from the pair distribution functions of Na⁺ and K⁺

	Na ⁺		K ⁺	
	First peak	<i>n(r)</i>	First peak	<i>n(r)</i>
GTH	2.40	5.00	2.70	5.41
MT	2.50	4.84	2.75	5.91
Marrone et al. [61]	2.55	5.5	2.95	6
Kim [29]	2.5	6.0	2.7	6.1

GTH and MT refer to the present calculations with different pseudopotentials. The last two lines refer to classical MD simulations

It can be seen from Fig. 2 that the distance of the first peak in $g(r)$ increases with increasing ionic radius; this will lead to an increase of the coordination number as it is actually found and summarized in Table 3. Other interesting features of the pair radial distribution functions are the broadening and lowering of height of the first peak in going from Li⁺ to Na⁺ and K⁺. The latter features are associated with a reduced strength of the interaction. The broadening of the first peak in $g(r)$ implies a higher possibility of penetration in the potential energy well and therefore a higher mobility of the solvent molecules with increasing radius of the ion [62]. In fact, it can be recalled that the $g(r)$ is related to the mean field potential [63] and gives therefore an indirect information on the average strength of the interaction. A more precise description of the mobility of the solvent cage is obtained considering the residence time of the solvent molecules in the first solvation shell. Li⁺ and Na⁺ interact with 4 and 5 molecules, respectively, in a stable way, i.e., the molecules reside in the solvation shell permanently all along the simulation time [22, 64, 32, 65]. The estimated lifetime of the molecules in the first solvation shell is in the case of Na⁺ greater than 8 ps and of ~5.2 ps for the K⁺ case, see Fig. 3. In the case of K⁺ the larger amplitude of motion is associated with diffusion and with an exchange of the solvent molecules in the first and second solvation shell. Figure 3 identifies as a function of time the molecules bound to K⁺ in the first

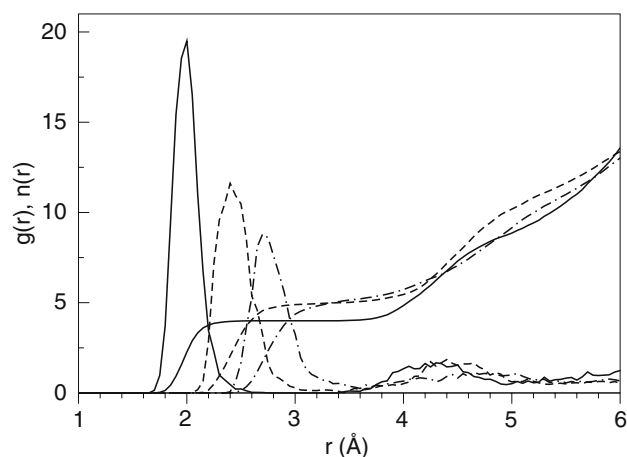


Fig. 2 Pair distribution functions and relative integration numbers for the $\text{O}\cdots\text{M}^+$ contacts; full lines $\text{M}=\text{Li}$; dashed lines $\text{M}=\text{Na}$; dotted-dashed lines $\text{M}=\text{K}$

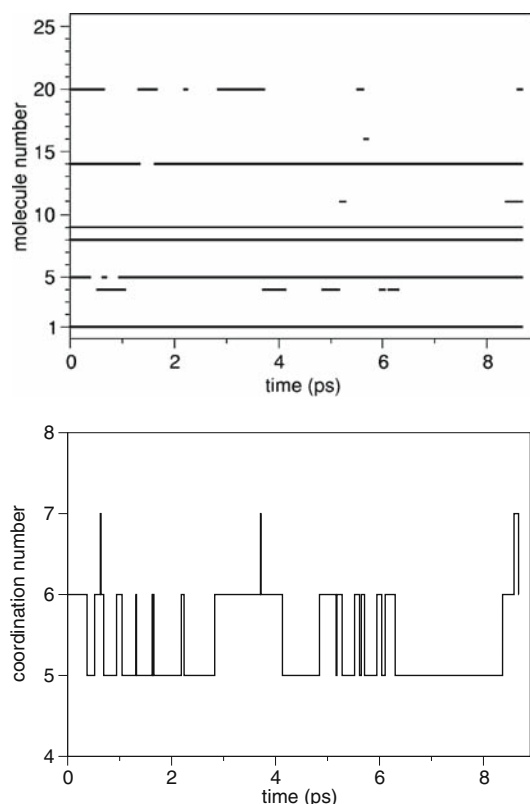


Fig. 3 Top panel Life time for $\text{O}\cdots\text{K}^+$ contacts. Each line means how long a molecule remains inside the first minimum distance (3.80 \AA) of the $g(r)$ and belongs to the first solvation shell. Molecules 1, 8 and 9 are always bonded ($t = 8.68 \text{ ps}$), molecules 14 and 5 are almost always bonded (8.37 and 8.18 ps respectively), molecules 20, 4 and 11 have a short residence time (2.11, 1.56 and 0.41 ps, respectively), and molecule 16 is bonded for only 0.06ps. The average residence time is about 5.2ps. In the bottom panel the instantaneous coordination number is reported

solvation shell. A molecule is defined to belong to the first solvation shell if the distance of its oxygen atom from the K^+ ion is smaller than the first peak position in the $g(r)$ function. It can be seen that molecules numbered 1, 8 and 9 are permanently in the shell, molecules 5 and 14 are almost constantly in the shell and other molecules alternate as first neighbors. The overall balance leads to a coordination number of 5.41. This can be attributed to the larger ionic radius of K^+ that allows, on average, a higher number of first neighbor solvent molecules.

Recently some papers [66,67] have been reported that widely used functionals may not be sufficiently accurate to describe the interactions of alkaline ions. As a further test of the degree of accuracy of our calculations and to check that the exchange of first neighbors, in the case of K^+ , is not due to the choice of the BLYP functional we have extracted randomly from the simulation three cluster configurations characterized by 5, 6 and 7 methanol molecules in the first solvation shell and computed the average binding energy at different levels of theory. The results reported in Table 4 show that all calculations have the same trend of the average binding energy with increasing coordination number. The calculations with B3LYP and PW91 functionals are closer to the MP2 results with respect to BLYP that gives slightly lower values. Two set of values are reported for the CPMD calculations using plane waves, one with periodic boundary conditions and the same cubic box adopted during the simulations and a second computed for an isolated system and more suited for comparison with the other calculations of Table 4. Even if the results of the latter are smaller than at the MP2 level, the differences are smaller than the required accuracy of our calculations.

A three-dimensional description of the motion of the Na^+ and K^+ ions around the solvent molecules is shown in Fig. 4, through the spatial distribution functions [69–72]. The isosurface close to the methanol molecule represents the probability to find the ion in a certain position, giving a clear representation of the mobility of the solvation cage. As expected, at the same isosurface value (in our case each point has to be visited 100 times), the K^+ ion spans a larger configurational phase space than the Na^+ ion.

The average structure of the solvent is not appreciably perturbed by the presence of the ions; as expected, the first peak of the $g(r)$ for the O–O contact is for both solutions 2.75 \AA and for the $g(r)$ for the O–D contact is at 1.80 \AA , in perfect agreement with the results obtained with the same model for the pure solvent [39].

A picture of the electronic rearrangement in the solution is obtained from the calculation of the electric dipole moment of the first shell methanol molecules. The dipole moment has been obtained from the positions of the maximally localized WFCs. [55,56] In Fig. 5 a snapshot of the WFCs for the Na^+ solvation shell is shown.

Table 4 Energies in kJ/mol, the calculations labelled BLYP, B3LYP, PW91 and MP2 were performed with the 6-311++G(d,p) basis set using the Gaussian suite of programs [68]

n	CPMD(pbc)	CPMD	BLYP	B3LYP	PW91	MP2
5	−61.04	−52.4919	−54.8544	−57.5523	−57.4253	−57.975
6	−57.73	−49.2533	−51.8116	−54.8043	−54.2518	−55.0805
7	−56.87	−48.7523	−50.4161	−53.3785	−52.5615	−53.6865

Fig. 4 Spatial distribution functions for Na^+ (a) and K^+ (b)

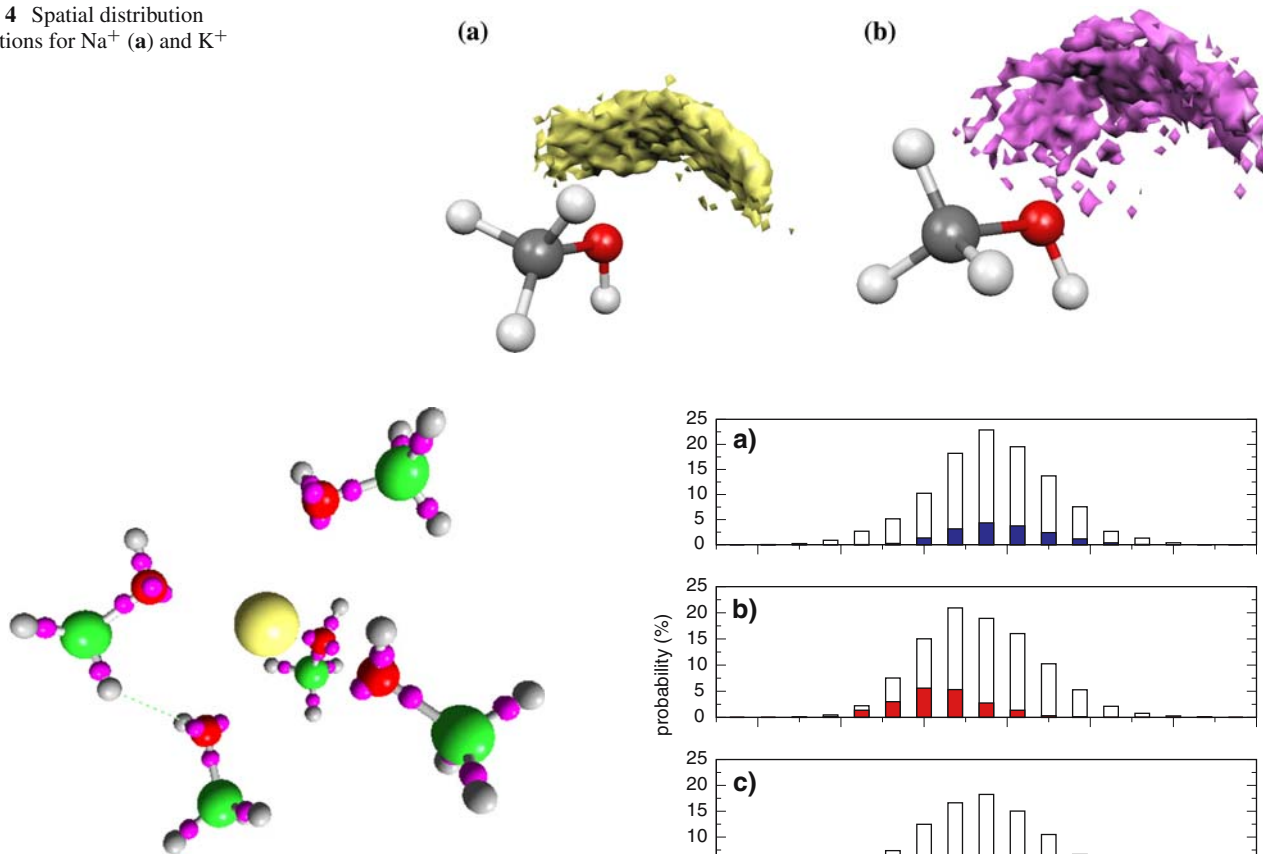


Fig. 5 Snapshot of the WFCs for Na^+

The distribution of the methanol molecule's dipole moment in the solution of the three ions is reported in Fig. 6, where the distribution in the whole solution and in the first solvation shell is compared. The average values of the dipole moment are summarized in Table 5.

In the Na^+ and K^+ solutions the distribution in the first solvation shell is ~ 0.2 D lower than in the whole solution. This situation is quite different than found for Li^+ , where $\langle \mu \rangle_{\text{tot}} \simeq \langle \mu \rangle_{\text{fs}}$. As a whole the behaviors of Na^+ and K^+ are similar and the charge transferred to the ions are almost identical ($-0.106 e^-$ and $-0.108 e^-$, respectively) and approximately half the value found for Li^+ . Therefore, the solvent molecules in Na^+ and K^+ solutions are much less polarized than in Li^+ .

An interesting picture of the charge redistribution in the solution can be obtained with the AIM method [58,59]. The results as a function of the ion–oxygen of the solvent mole-

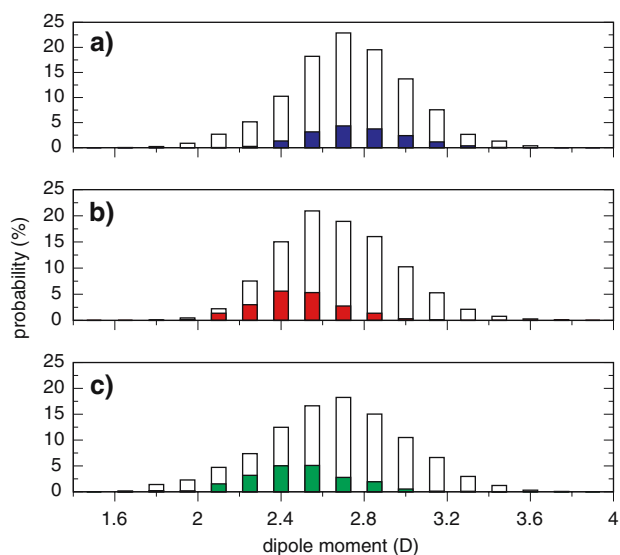


Fig. 6 Dipole moment distribution (in debye, D) for: a Li^+ , b Na^+ , c K^+ ; the colored bars refer to the dipole moment distribution of the first solvation shell molecules

Table 5 Average dipole moment values (in debye, D) and relative standard deviation for the solution ($\langle \mu \rangle_{\text{tot}}$) and for the first shell molecules contribution ($\langle \mu \rangle_{\text{fs}}$).

	$\langle \mu \rangle_{\text{tot}}$ D	$\langle \mu \rangle_{\text{fs}}$ D
Li^+ [22]	2.73	2.76
Na^+	2.67 ± 0.28	2.48 ± 0.21
K^+	2.66 ± 0.34	2.49 ± 0.26

cules distance are reported in Fig. 7. The behavior is similar to that reported for the Na^+ and K^+ ions in water [73].

The already discussed transfer of negative charge from the first shell molecules to the ions is more than counterbal-

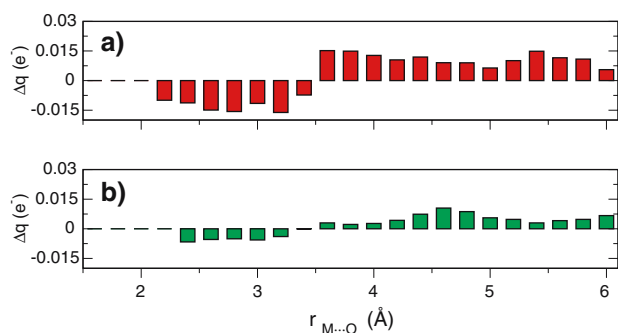


Fig. 7 Transferred electronic charge distribution $\Delta q(e^-)$, as a function of the distance between the ion and the oxygen atom of methanol molecules $r_{M...O}$; the reported values are integrated on a sphere: **a** $M=Na^+$; **b** $M=K^+$. For Na^+ and K^+ the graphs are reported as a function of the M–O distance. The integrated charge in the first solvation shell is $-0.063e$ and $-0.057e$ for Na^+ and K^+ , respectively. The integrated charge outside the first solvation shell amounts to $0.168e$ and $0.163e$ for Na^+ and K^+ , respectively. The sum of these two terms balances the charge transferred to the ion with an uncertainty on the third decimal place.

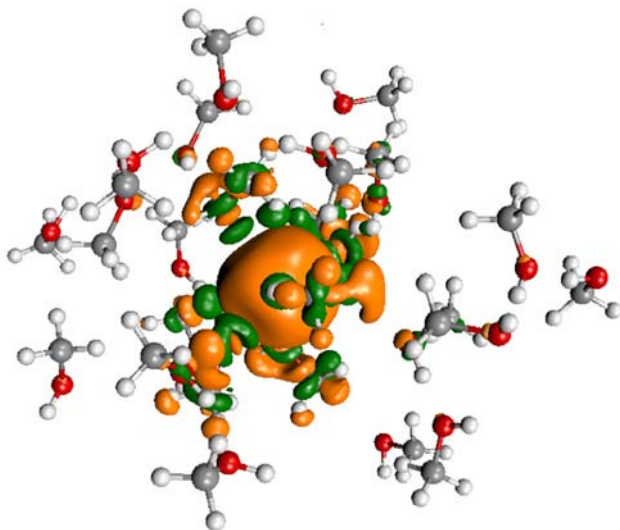


Fig. 8 Electronic density flux for a selected configuration. The decrease and the increase in electronic density are reported in *green* and *orange*, respectively

anced by a charge transfer from the outer to the first shell molecules through the hydrogen bond network. As a net balance the positively charged ion is surrounded by a negatively charged first shell and a positively charged second shell. A qualitative view is confirmed by Fig. 8 that reports the flux of electronic density.

This charge alternation contributes to the stability of the cage structure and to a tighter reorganization of the solvent. It can be seen from Fig. 7 and Table 6 that the stability of the first solvation shell for Li^+ is enhanced by the larger charge transfer.

Table 6 Transferred electronic charge amount $\Delta q(e^-)$ on ions and relative standard deviation

	$\Delta q(e^-)$
Li^+ [22]	$\cong -0.2$
Na^+	$-0.106 \pm 7.34 \times 10^{-3}$
K^+	$-0.108 \pm 6.89 \times 10^{-3}$

Conclusions

Ab initio CPMD simulations have been performed on Na^+ and K^+ ions in liquid methanol to obtain several details on the structure and electronic properties of the first solvation shell. The reliability of this approach in modelling the ion–methanol interaction has been confirmed comparing the results with calculations with a localized Gaussian basis set at the MP2 level of theory. It has been shown that simple cations are strongly bound to the methanol molecules of the first solvation shell forming a stable cage. AIM population analysis has shown that charge transfer from the first shell methanol molecules to the ions is more than balanced by the charge transfer from methanol molecules of the second shell such that the first solvation shell molecules are negatively charged. This contributes to stabilize the cage. It has been confirmed that the methanol molecules in the first solvation shell are characterized by an “orientation order” with the lone pairs of the oxygen atom pointing toward the ion [25,27], as reported in Fig. 5 for Na^+ , but a similar behavior occurs for K^+ . The polarization of the solvent molecules has been studied through the WFCs analysis. By comparison with the pure solvent [39] it appears evident that the perturbation due to the ions is mainly limited to the first solvation shell [24]. The stability of the cage will affect colligative properties of the solution, eliminating the molecules of the first solvation shell, and the diffusion properties of the ions since the molecules of the first solvation shell will diffuse with the ion increasing their effective radius. This stability will also have consequences on the reactivity of these species in solution.

Acknowledgements This work was supported by the Ministero dell’Istruzione, dell’Università e della Ricerca (MIUR).

References

- Ohtaki H, Radnai T (1993) Chem Rev 93: 1157–1204
- González BS, Hernández-Rojas J, Wales DJ (2005) Chem Phys Lett 412: 23–28
- Kropman MF, Bakker HJ (2001) Science 291: 2118–2120
- Omta AW, Kropman MF, Bakker SWHJ (2003) Science 301: 347–349
- Hamm P, Lim M, Hochstrasser RM (1998) Phys Rev Lett 81: 5326–5329

6. Guillot B, Marteau P, Obriot J (1990) *J Chem Phys* 93: 6148–6164
7. Spångberg D, Hermansson K (2004) *Chem Phys* 300: 165–176
8. Spångberg D (2003) Cation solvation in water and acetonitrile from theoretical calculations PhD thesis, Uppsala
9. Spångberg D, Hermansson K (2003) *J Chem Phys* 119: 7263–7281
10. Spångberg D, Rey R, Hynes JT, Hermansson K (2003) *J Phys Chem B* 107: 4470–4477
11. Jancsó G, Bopp P, Heinzinger K (1985) *Z Naturforsch* 40: 1235
12. Smith DE, Dang LX (1994) *J Chem Phys* 101: 7873
13. Peslherbe G, Ladanyi B, Hynes J (2000) *J Phys Chem A* 104: 4533
14. Jorgensen WL, Severance DL (1993) *J Chem Phys* 99: 4233
15. Perera L, Berkowitz ML (1993) *Z Phys D* 26: 166
16. Brodskaya E, Lyubartsev AP, Laaksonen A (2002) *J Chem Phys* 116: 7879–7892
17. Vuilleumier R, Sprik M *J Chem Phys* 115(8): 3454–3468
18. Lavanya M, Bernasconi M, Parrinello M (1999) *J Chem Phys* 111: 1588–1591
19. Jardón-Valadez E, Costas M (2004) *J Mol Struct* 677: 227–236
20. Carignano MA, Karlström G, Linse P (1997) *J Phys Chem B* 101: 1142–1147
21. Carrillo-Tripp M, Saint-Martin H, Ortega-Blake I (2003) *J Chem Phys* 118: 7062–7073
22. Pagliai M, Cardini G, Schettino V (2005) *J Chem Phys B* 109: 7475–7481
23. Faralli C, Pagliai M, Cardini G, Schettino V (2006) *J Phys Chem B*, 110: 14923–14928
24. Jorgensen WL, Bigot B, Chandrasekhar J (1982) *J Am Chem Soc* 104: 4584–4591
25. Chandrasekhar J, Jorgensen WL (1982) *J Chem Phys* 77: 5080–5089
26. Mark D, Heinzinger K, Palinkas G, Bako I (1991) *Z Naturforsch* 46a: 887–897
27. Selegue TJ, Moe N, Draves JA, Lisy JM (1992) *J Chem Phys* 96: 7268–7278
28. Guàrdia E, Pinzón R (2000) *J Mole Liq* 85: 33–44
29. Kim HS (2001) *J Mole Struct (Theochem)* 540: 79–89
30. Krienke H, Fischer R, Barthel J (2002) *J Mol Liq* 98(99): 329–354
31. Impey RW, Sprik M, Klein ML (1987) *J Am Chem Soc* 109: 5900–5904
32. Sesé G, Guàrdia E, Padró JA (1996) *J Chem Phys* 105: 8826–8834
33. Sesé G, Guàrdia E, Padró JA (1998) *J Chem Phys* 108: 6347–6352
34. Chandrasekhar J, Spellmeyer D, Jorgensen W (1984) *J Am Chem Soc* 106: 903–910
35. Robertson WH, Johnson MA (2003) *Annu Rev Phys Chem* 54: 173–213
36. Sprik M, Klein ML, Watanabe K (1990) *J Phys Chem* 94: 6483–6488
37. Car R, Parrinello M (1985) *Phys Rev Lett* 55: 2471–2474
38. Tse JS (2002) *Ann Rev Phys Chem* 53: 249–290
39. Pagliai M, Cardini G, Righini R, Schettino V (2003) *J Chem Phys* 119: 6655–6662
40. Handgraaf J-W, van Erp TS, Meijer EJ (2003) *Chem Phys Lett* 367: 617–624
41. Morrone JA, Tuckerman ME (2002) *J Chem Phys* 117: 4403–4413
42. Tongraar A, Liedl KR, Rode BM (1998) *J Phys Chem A* 102: 10340–10347
43. White JA, Schwegler E, Galli G, Gygi F (2000) *J Chem Phys* 113: 4668–4673
44. Ramanih LM, Bernasconi M, Parrinello M (1999) *J Chem Phys* 111: 1587–1591
45. Hutter J, Alavi A, Deutch T, Bernasconi M, Goedecker S, Marx D, Tuckerman M, Parrinello M (1995–1999) CPMD, MPI für Festkörperforschung and IBM Zurich Research Laboratory, Stuttgart
46. Troullier N, Martins JL (1991) *Phys Rev B* 43: 1993–2006
47. Kleinman L, Bylander DM (1982) *Phys Rev Lett* 48: 1425–1428
48. Krack M (2005) *Theor Chem Acc*, 114: 145–152
49. Goedecker S, Teter M, Hutter J (1996) *Phys Rev B* 54: 1703–1710
50. Hartwigsen C, Goedecker S, Hutter J (1998) *Phys Rev B* 58: 3641–3662
51. VandVondele J, Mohamed F, Krack M, Hutter J, Sprik M, Parrinello M (2005) *J Chem Phys* 122:(014515)
52. Becke AD (1988) *Phys Rev A* 38: 3098–3100
53. Lee C, Yang W, Parr RG (1988) *Phys Rev B* 37: 785–789
54. Frisch MJ, Trucks GW, Schlegel HB, Scuseria GE, Robb MA, Cheeseman JR, Zakrzewski VG, Montgomery Jr. JA, Stratmann RE, Burant JC, Dapprich S, Millam JM, Daniels AD, Kudin KN, Strain MC, Farkas O, Tomasi J, Barone V, Cossi M, Cammi R, Mennucci B, Pomelli C, Adamo C, Clifford S, Ochterski J, Petersson GA, Ayala PY, Cui Q, Morokuma K, Malick DK, Rabuck AD, Raghavachari K, Foresman JB, Cioslowski J, Ortiz JV, Stefanov BB, Liu G, Liashenko A, Piskorz P, Komaromi I, Gomperts R, Martin RL, Fox DJ, Keith T, Al-Laham MA, Peng CY, Nanayakkara A, Gonzalez C, Challacombe M, Gill PMW, Johnson B, Chen W, Wong MW, Andres JL, Gonzalez C, Head-Gordon M, Replogle ES, Pople JA, Gaussian 98, Revision A.11, Gaussian Inc., Pittsburg, PA, 1998
55. Marzari N, Vanderbilt D (1997) *Phys Rev B* 56: 12847–12862
56. Silvestrelli PL, Marzari N, Vanderbilt D, Parrinello M (1998) *Solid State Comm* 107: 7–11
57. Berghold G, Mundy CJ, Romero AH, Hutter J, Parrinello M (2000) *Phys Rev B* 61: 10040–10048
58. Bader RFW (1990) *Atoms in Molecules—a quantum theory*, Oxford University Press, Oxford
59. Bader RFW (1991) *Chem Rev* 91: 893–928
60. Szeferczyk B, Sokalski WA, Leszczynski J (2002) *J Chem Phys* 117: 6952–6958
61. Marrone TJ, Merz KM Jr (1993) *J Phys Chem* 97: 6524–6529
62. Shannon RD (1976) *Acta Cryst A* 32: 751–767
63. Chandler D (1987) *Introduction to modern statistical mechanics*, Oxford University Press, New York
64. Lee SH, Cummings PT (2000) *J Chem Phys* 112: 864–869
65. Hawlicka E, Swiatla-Wojcik D (2002) *J Chem Phys A* 106: 1336–1345
66. Westphal E, Josefredo R, Pliego Jr (2005) *J Chem Phys* 123: 074508
67. Ho DS, DeYonker NJ, Wilson AK, Cundari TR (2006) *J Phys Chem A* 110: 9767
68. Frisch MJ, Trucks GW, Schlegel HB, Scuseria MARGE, Cheeseman JR, Montgomery Jr., JA, Vreven KNKT, Burant JC, Millam JM, Iyengar SS, Tomasi VBJ, Mennucci B, Cossi M, Scalmani G, Rega GAPN, Nakatsuji H, Hada M, Ehara M, Toyota RFK, Hasegawa J, Ishida M, Nakajima T, Honda Y, Kitao HNO, Klene M, Li X, Knox JE, Hratchian HP, Cross CAJB, Jaramillo J, Gomperts R, Stratmann RE, Yazyev AJAO, Cammi R, Pomelli C, Ochterski JW, Ayala KMPY, Voth GA, Salvador P, Dannenberg VGZJJ, Dapprich S, Daniels AD, Strain OFMC, Malick DK, Rabuck AD, Raghavachari JBFK, Ortiz JV, Cui Q, Baboul AG, Clifford JCS, Stefanov BB, Liu G, Liashenko A, Piskorz IKP, Martin RL, Fox DJ, Keith T, Al-Laham CYPMA, Nanayakkara A, Challacombe M, Gill BJPMW, Chen W, Wong MW, Gonzalez C, Pople JA (2004) *Gaussian 03, Revision C.02*, Gaussian Inc, Wallingford CT,
69. Svishchev IM, Kusalik PG (1993) *J Chem Phys* 99: 3049–3058
70. Svishchev IM, Kusalik PG (1994) *J Chem Phys* 100: 5165–5171
71. Khalack JM, Lyubartsev AP (2005) *J Chem Phys* 109: 378–386
72. de la Peña LH, Kusalik PG (2005) *J Am Chem Soc* 127: 5246–5251
73. Dal Peraro M, Raugei S, Carloni P, Klein ML (2005) *Chem Phys Chem* 6: 1715–1718